4.5.2. SEISMOTECTONICS OF WESTERN GREECE USING GEOPHYSICAL AND SEISMOLOGICAL DATA

Alexandros Stampolidis, Gregory Tsokas, Anastasia Kiratzi

4.5.2.1. Introduction

The area of western Greece, a seismically active region, exhibits substantial tectonic complexity mainly dominated by the counter clockwise motion of the Apulia microplate in the north and the active subduction of the front part of the African plate beneath Eurasia, in the south (Papazachos, Comninakis, 1970, 1971). Later studies on the crustal and upper mantle velocity structure by tomographic methods (Spakman, 1986, Papazachos et al., 1995, Papazachos, Nolet, 1997) fully supported the idea of the subduction in the southern Aegean area. Tsokas and Hansen (1997) constructed a model of the subducting lithosphere. They used the frequency domain method of Hansen and Wang (1988) to compute its gravity effect.

The present study aims to the identification of the location, depth, strike and dip of gravity contacts in the region of western Greece and southern Albania, which are interpreted to present structural boundaries. We follow the foundation and terminology of the work of Thurston and Smith (1997). They formed an automatic interpretation scheme for the magnetic data, based on the complex attributes which they named "Source Parameter Imaging (SPI^{TM})" method. We use the code developed by Philips (1997) for the calculation of the source parameters.

Available complete Bouguer gravity anomaly data from western Greece and southern Albania were combined to produce the gravity map of the study area. The available Moho depths for the region were used to compute the gravity effect of the crust and, along with the effect of the subducting slab from Tsokas and Hansen (1997), were subtracted from the data. The residual gravity field is depictive of the shallow features in the region. Linear features on the residual map, that run for hundreds of kilometres, commonly represent major crustal shear zones and faults. The potential-field manifestation of a fault may vary along its trend, depending on the local geology, so alignments of discontinuous multiple local anomalies are of interest. The results of the potential field studies are interpreted jointly with the seismological data.

4.5.2.2. Seismotectonic setting

Fig. 4.5.2.1 presents the distribution of shallow seismicity in Greece which is concentrated in east-trending and northeast-trending zones of deformation. Most shallow earthquakes in central and northern Greece (h<50 km) result from the interaction between Eurasia plate and the small Aegean Sea plate, which is moving southwest with respect to the Eurasia plate with a velocity of about 30 mm/year (McClusky et al., 2000).

The boundary between the Aegean plate and the Eurasia plate in central and northern Greece is diffuse (Jackson, 1994). A belt of shallow-focus seismicity along the western

coast of Greece to the north of Lefkada, and extending north along the Adriatic coast of the Balkan Peninsula, is characterized by reverse fault earthquakes occurring in response to northeast-southwest crustal convergence. This zone produced an earthquake of magnitude 7.0 in 1979, beneath the coast of Montenegro (Anderson, Jackson, 1987, Baker et al., 1997). In the twentieth century, the largest shallow-focus earthquakes to have occurred near the Hellenic-arc plate boundary had magnitudes of about 7.2. Historical sources and archaeological studies suggest that earthquakes near Crete in 365 AD and 1303 AD may have been much larger than any Hellenic arc earthquake of the twentieth century (Papazachos, Papazachou, 2003). Shallow-focus earthquakes also occur in the volcanic arc that is associated with the subduction of the African plate beneath the Aegean Sea plate, in the Dodecanese and Cyclades Islands, over 100 km north of Crete.

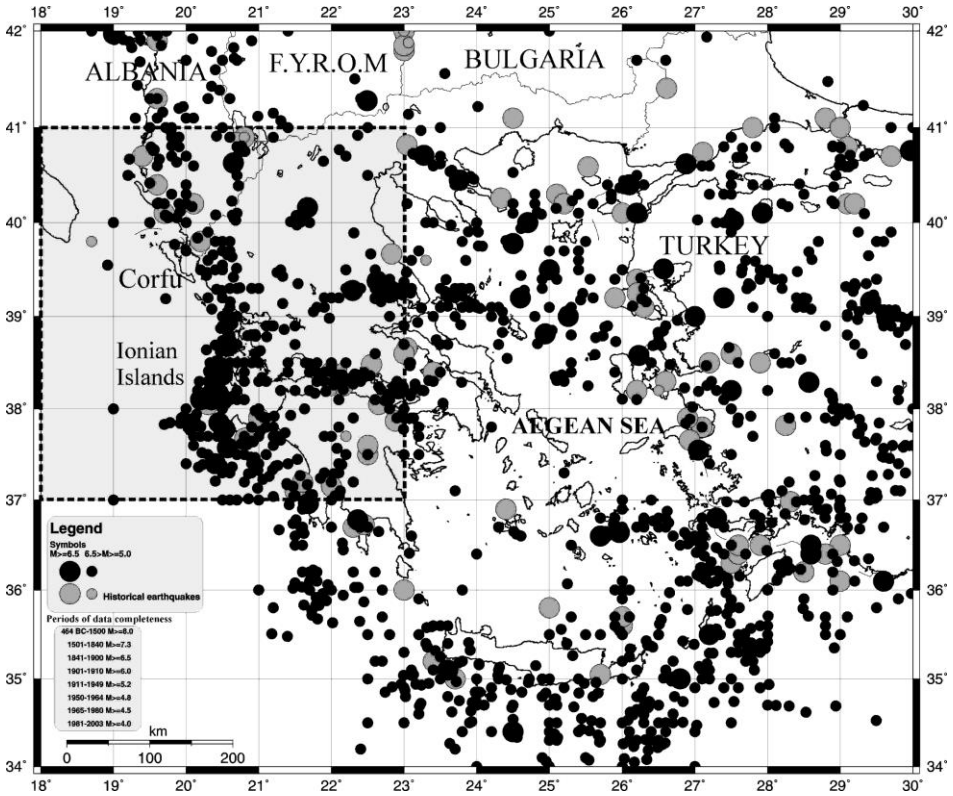

Fig. 4.5.2.1. Distribution of shallow seismicity in Greece. Epicentre locations are as listed in the catalogue of the Geophysical Laboratory of the Aristotle University of Thessaloniki. The completeness threshold of the data and the corresponding periods are shown in the legend. The area we specifically study here is included in the grey rectangle.

The distribution of focal mechanisms in the region of study (Fig. 4.5.2.2) shows that the east-trending zones, most prominent in mainland Greece, are characterized by predominantly normal faulting. The northeast-trending belts are characterized by predominately strike-slip fault earthquakes (Kiratzi, 2002). The collision zone of coastal Albania – NW coastal Greece up to the island of Lefkada has been well defined in the past (i.e Papazachos et al., 1998, Louvari et al., 1999, 2001, Kiratzi, Louvari, 2003 and references therein). Off the west coasts of Cephalonia and Lefkada Islands, western

Greece, strike – slip faulting is prevailing (Scordilis et al., 1985, Louvari et al., 1999, Louvari, 2000, Benetatos et al., 2005).

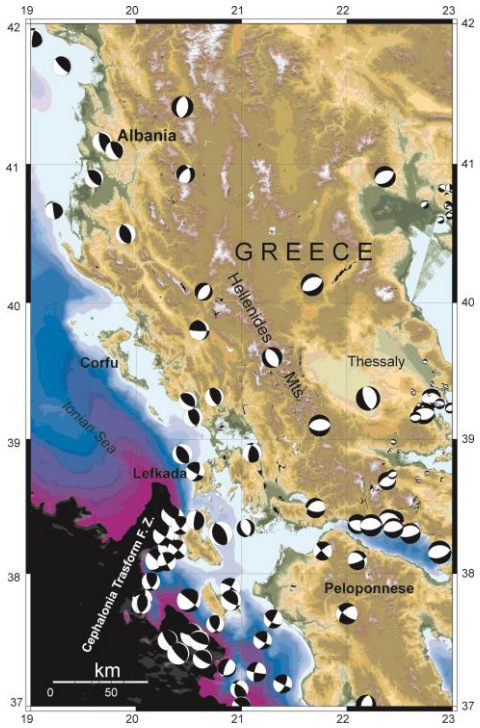

Fig. 4.5.2.2. Earthquake focal mechanisms in western Greece. Black quadrants denote compression and white quadrants denote dilatation. Note the zone of low- angle thrusting along the coast of Albania and western Greece, the strike – slip motions in the Cephalonia Transform Fault Zone and the normal faulting in the back – arc area.

The reverse – low angle thrust faulting connected to the Hellenic trench is recognized to start ~50 km S of Zante and follows the bathymetric expression of the Hellenic Trench (from Peloponnese to Crete, along off – coast of Crete, east of Karpathos and Rodos up to southern Turkey). Most of the focal mechanisms (shown in Fig. 4.5.2.2.) indicate that western Peloponnese (from Patras up to the Gulf of Kyparissia) is deforming by strike-slip faulting an observation previously made in Papazachos et al. (1998). In addition the entire region that extends from the Gulf of Kyparissia up to the island of Zante and the deformation of Zante itself seems to be connected with strike-slip motions.

4.5.2.3. Source of geophysical data and processing method

Fig. 4.5.2.3 shows the complete Bouguer gravity anomaly map of the area under study, as it was extracted from the gravity database of the University of Athens (Lagios et al., 1996). The unit cell of this database is 4 km which reflects approximately the average station density of the initial data set of Makris and Stavrou (1984). The Bouguer anomaly map of Albania was recompiled (Kane, 2003) from gravity data measured between 1950 and 1990 by the Albanian geophysical companies of Tirana and Fier. Kane (2003) tried to combine this data set with the Greek database, by shifting the Albanian data and filtering them at the border region.

Regional/residual separation was the next step in our processing layout. Following Tsokas and Hansen (1997) we constructed a new Moho depth map for western Greece and Albania by combining the depth data from of the work of Tsokas and Hansen

(1997) for Greece and Papazachos et al. (2005) for Albania, and calculated the gravity effect of the crust. The new Moho depth map formed the lower surface of the model that approximate the crust, while the upper surface was a plane at the sea level. The frequency domain method of Parker (1973) and its implementation by Blakely (1981) were used for the calculation. The average density contrast between upper mantle and crust was set to $\delta\rho=0.35 gr/cm^3$. Furthermore, we added the gravity effect of the subducting African slab under the Aegean microplate calculated by Tsokas and Hansen (1997) to the effect of the crust to compute the regional gravity field of the study area.

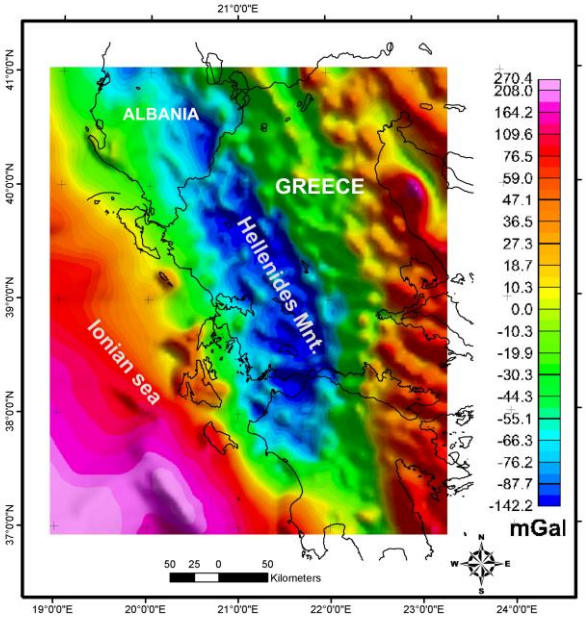

Fig. 4.5.2.3. The complete Bouguer gravity anomaly map of the area under study

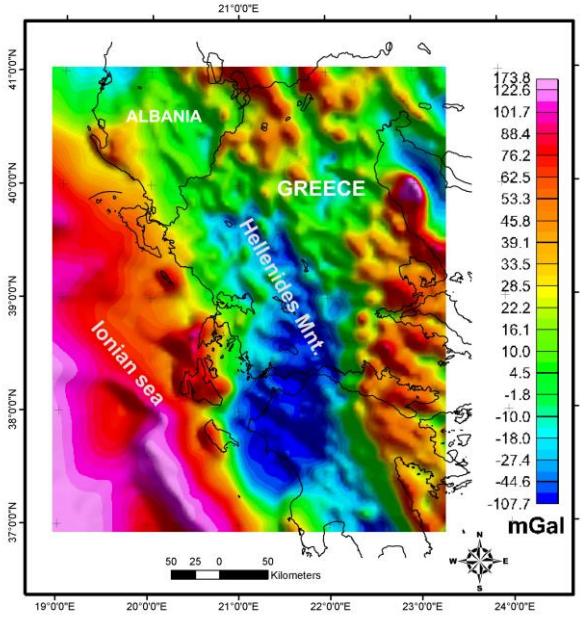

Fig. 4.5.2.4. Residual gravity map after the subtraction of the crust and the subducting lithosphere gravity effects from the Bouguer map

The residual gravity map (Fig. 4.5.2.4.) was the result of subtracting the regional field from the complete Bouguer anomaly map. This map is in fact the isostatic residual map. The residual gravity field is characterized by local anomalies caused by relative shallow features in the region, which mainly reflect the geological and tectonic structure of the area.

4.5.2.4. Method of complex attributes analysis

Nabighian (1972) introduced the simple analytic signal A in the geophysical literature. He defined A, of a 2D magnetic anomaly in two ways: 1) in terms of horizontal and vertical derivatives and 2) in terms of the total field and its Hilbert transforms. The former definition is:

(1)
$$A(x,y)=\frac{\partial M(x,z)}{\partial x}-j\frac{\partial M(x,z)}{\partial z}$$

where M(x,z) is the magnitude of total magnetic field, j is the imaginary unit, z and x are the Cartesian coordinates for the vertical direction and the direction perpendicular to the strike. The simple analytic signal *A*, or "energy envelope" of a three-dimensional magnetic or gravity anomaly is defined as

(2)
$$A(x,y)=\left(\frac{\partial T}{\partial x}\hat{x}+\frac{\partial T}{\partial y}\hat{y}+i\frac{\partial T}{\partial z}\hat{z}\right)$$

where *T* is the total magnetic field, *i* is the imaginary number and $\hat{x}$, $\hat{y}$, $\hat{z}$ are unit vectors in Cartesian coordinates. The real and imaginary parts of Eq.2 form a Hilbert transform pair, which allows the vertical derivative to be easily calculated in the frequency domain when horizontal derivatives in two perpendicular directions are available (Nabighian, 1984, Roest et al., 1992).

The amplitude and local phase of the simple analytic signal in three dimensions are given by Roest et al., (1992)

(3)
$$|A(x,y)|=\sqrt{\left(\frac{\partial T}{\partial x}\right)^2+\left(\frac{\partial T}{\partial y}\right)^2+\left(\frac{\partial T}{\partial z}\right)^2}$$

and

(4)
$$\Theta=\tan^{-1}\left(\frac{\frac{\partial T}{\partial z}}{\sqrt{\left(\frac{\partial T}{\partial x}\right)^2+\left(\frac{\partial T}{\partial y}\right)^2}}\right)$$

The local wavenumber method comes from The Source Parameter Imaging (SPI) method (Thurston, Smith, 1997), which extends the theory of the simple analytic signal by computing three complex attributes from which source parameters can be calculated. In the case of spatial magnetic data, these attributes include the local amplitude (analogous to the analytic signal amplitude), local phase and local wavenumber. The local wavenumber *k* is defined as the rate of change of the local phase *Θ* of the total field *T* with respect to the horizontal (*x* and *y*) directions and can be expressed (Thurston and Smith, 1997) as:

(5)
$$k=\sqrt{\left(\frac{\partial\Theta}{\partial x}\right)^2+\left(\frac{\partial\Theta}{\partial y}\right)^2}$$

The local wavenumber, like the analytic signal, peaks over magnetic contacts and is independent of the regional magnetic field direction, the source magnetization and the dip of the contact (Thurston, Smith, 1997). The theoretical shape of the two dimensional local wavenumber over a contact is given by

(6) $$k = \frac{d}{h^2 + d^2}$$

with *h* being the horizontal distance to the contact and *d* the depth to the top of the contact. From this equation it, it is easily seen that directly over a contact the depth *d* to the top of the contact with infinite depth extent is the inverse of the peak value of the local wavenumber (Thurston, Smith, 1997). Phillips (1997) suggested that taking the vertical integral of the total magnetic field before calculating the local wavenumber would improve depth results for contacts with a finite thickness.

This method can be applied to gridded magnetic or gravity data. Higher order derivatives are calculated in the frequency domain. The appropriate equation is solved for the local wavenumber at each grid point, and a new grid containing the local wavenumber is created. Crests in the local wavenumber are then found by passing a 5×5 data window over the newly created grid and searching for local maxima. When a crest is found and its local strike direction is determined, the source depth and its standard error are estimated by a least-squares fit perpendicular to strike to the theoretical shape of the two-dimensional local wavenumber over a contact.

4.5.2.5. Application Results

The processing of complex attributes analysis in the area of western Greece was realized on the residual Bouguer gravity map. Complex attributes analysis requires higher order derivatives. An accurate calculation of higher order derivatives is often difficult when data contain noise. We upward continued the data in the frequency domain (Hildenbrand, 1983) by one grid cell (4 km) to reduce noise, prior to any other processing, following Phillips (2001 and references therein).

The local wavenumber method is usually applied to magnetic data while gravity data have to be transformed to equivalent magnetic data using the pseudomagnetic transformation. We computed the "local source parameters" of the residual upward continued gravity field by applying the local wavenumber method to the pseudomagnetic transformation grid. The local wavenumber grid, the local phase grid and local amplitude grid were computed automatically. Then we used them to calculate the source parameters which include the position, depth, strike, dip angle, dip azimuth, and physical property contrast of a computed contact, as shown in Fig. 4.5.2.5 a. Tsokas (2000) and Gettings and Houser (2000) applied the local wavenumber method on complete Bouguer gravity data. We implement the method on the residual upward continued gravity field and the results are shown in Fig. 4.5.2.5 b.

The local estimates depicted in Fig. 4.5.2.5 a, b denote that the shallow structures who cause the gravity anomalies follow a NW- SE trend along the coastal western Greece and Ionian Sea. This is in accordance with the geometry of the Hellenic arc at this geographic latitude.

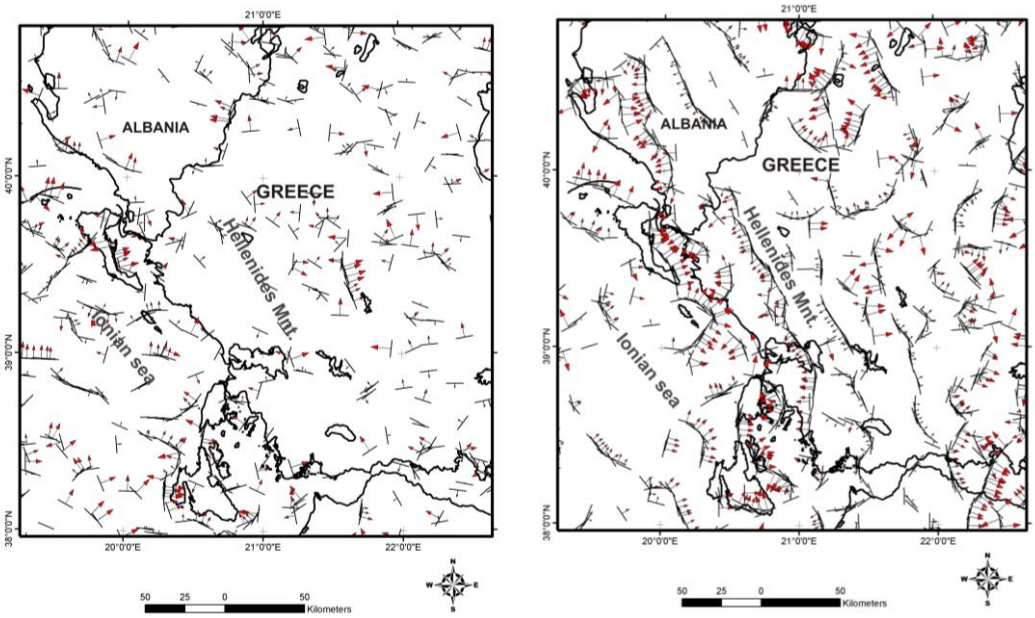

a) **b)**

Fig. 4.5.2.5. Trends and dips for sources of gravity anomalies computed from a) the pseudomagnetic transformation of the residual upward continued Bouguer gravity anomaly grid and b) from the residual upward continued Bouguer gravity anomaly grid. Trends are shown with black line segments, while dips are shown with red headed arrows. The length of the arrow is proportional to its contact dip angle.

4.5.2.6. Discussion and conclusions

We have used complex attributes analysis on the gravity data of western Greece and Albania, in order to infer the characteristics of the major structural features. In Fig. 4.5.2.6 we combine the tectonic lineaments as inferred from the geophysical data with other structures of the area concluded by the regional geological and tectonic setting of the area plus the studies of the seismological regime. The boundaries of the major geological zones of Greece and Albania are depicted with green colour. Red and blue line segments denote the trends of structures as inferred from the geophysical data. The yellow straight lines denote the seismogenic faults that are known to have rupture in the past (Papazachos et al., 2001). On the same figure the shallow seismicity is also plotted with the open circles.

First of all it is evident that the distribution of the local estimates coincides fairly well with large scale geologic structures, namely the borders of the major geological zones. They show the general NW – SE trend in continental Albania and the mainland of Greece. This fact implies that the zones have discernible mean densities, a fact that was more or less expected. Thus, their boundaries comprise perfect contacts absolutely confront able to the basic model used for the built up of the technique of complex attributes. In this context, besides the expected agreement between the geophysical estimates and the visible contacts of the zones, the results should be considered as very reliable for the cases where these contacts are concealed under sedimentary cover. The lineament, parallel to the Pindos thrust, mark with the letter A in Fig. 4.5.2.6. is such an example.

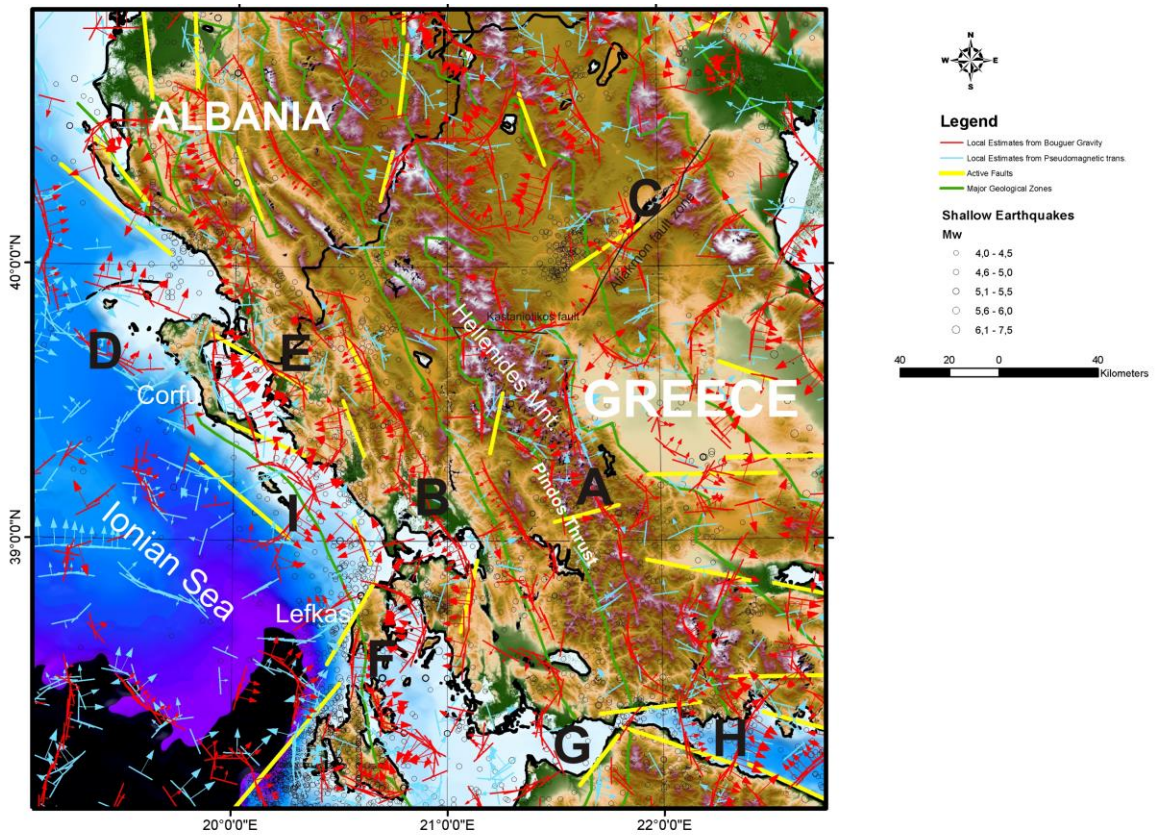

Fig. 4.5.2.6. Comparison of tectonic structures inferred from the geophysical data (red and blue line segments) with active seismic faults (yellow lines), boundaries of geological zones (green) and shallow seismicity (open circles). Letters are explained in the text.

The faults plotted with yellow lines in Fig. 4.5.2.6. are the surface projection of the traces of the active faults that produced strong earthquakes in Greece and are not necessarily connected with any surface expression. Actually, in Greece very few earthquakes have produced ruptures that reached the surface, and when they did so these traces were sometimes interpreted as secondary effects, due to gravity for instance or small fissures on the surface. Thus, one can say that many strong earthquakes in Greece are clearly connected with the rupture of blind thrust or normal faults. Moreover, offsets of many kilometers of major faults rarely occur on single surfaces but rather are accommodated across fault zones of a few kilometers. Thus, the structures depicted from the processing of geophysical data could be any kind of altered zones – fractures, faults or shear zones. The correlation with the recent active faults is not straightforward in most of the cases, due to the reasoning previously stated. More over, the complex attributes technique is designed such that subsurface contacts being detected and estimates of their characteristics being inferred. In other words, a subsurface contact more likely been created by a past tectonic event, is not necessarily related to the recent seismicity. The block segments depicted from geophysics are in better agreement with the common sense in terms of expected seismotectonics, especially along the coastal region of Albania and western Greece, where compressional tectonics occur along NW – SE trending structures.

The local estimates inferred from complex attributes analysis, as expected, delineate better the boundaries of the Hellenides and the general NW – SE trend of the Hellenic mountain chain. There is a big lineament trending approximately NNW-SSE which is parallel to the geological boundary between Ionian and Gavrovo zones. This feature has

been annotated by the letter B in Fig. 4.5.2.6 It's evident that the particular lineament does not coincide with any tectonic feature of the same size, but some parts of it coincide with two active faults. Therefore, this lineament is either reflecting the mountain chain which rises at about the same position or it reflects a concealed tectonic boundary partially exposed. The curved feature annotated as C follows the channel of Aliakmon River. It crosses almost perpendicular the Hellenides and it is caused by various faults, known as Aliakmon fault zone. This lineament passes from the region of Kozani – Grevena, the site of the 1995 Mw 6.6 earthquake, were the geologic boundaries are also well picked up by the used method.

Another lineament that coincides with major tectonic boundary has been annotated by the letter D. That particular one reflects the northern extension of the boundary between Ionian and Paxoi zones, NW of Corfu Isl. On the other hand, alignments of local estimates do show up in other locations some of which reflect known or unknown faults. In the mainland of continental Greece and especially in the eastern coastlines, where the active faults are often E – W trending normal faults (see Fig. 4.5.2.2) the correlation between geophysical anomalies and seismicity is very poor. The fault east of Corfu trending NW-SE is coincident with a lineament that extends further to the north, annotated as E in Fig. 4.5.2.6 The fault of Lixouri known to have been destructed from major shocks during the 20th century coincides with a lineament on Fig. 4.5.2.6 that is annotated as F. This lineament is parallel to the border of Ionian and Paxoi zones at the area.

Several alignments of estimates are observed to cross the Gulf of Corinth. This can be seen in the areas marked as G and H in Fig. 4.5.2.6. Evidently, they reflect the presence of concealed subsurface density contacts in the respective particular localities. In particular, the subsurface structures detected at the southeast corner of the map of Fig. 4.5.2.6, show opposing dips. The reflect means that a tectonic graben should present in this area. The referred features strike towards NE, near parallel to the boundaries of geological zones, while the known active faults in the area are parallel to the coastline.

This is an indication that the age of these features must represent tectonic structures older than the late Plio-Pleistocene extension (Van Hinsberger at al., 2005 and references herein) that resulted in the formation of the basins at the Gulf of Corinth and the Gulf of Patras. A similar situation is observed south of Paxoi Island. In fact, the alignments, marked as I in Fig. 4.5.2.6., produced by the study of the gravity field cross almost perpendicularly the boundary between Ionian and Paxoi zones, and also the fault concluded by the seismological data. Thus, pronounced strike discrepancies between the features concluded by different methods are observed in certain areas. These are most likely to reflect the presence of concealed gravity contacts who have neither surface expression nor they are responsible for any recent earthquake.

Most of the linear features at Ionian Sea follow the topography of the sea bottom, in an area that has neither shallow earthquakes nor active faults.

As a general conclusion we can say that the analysis followed here has shown very well the large scale geologic boundaries but does not correlate well with the small – scale faults that have not yet produced large offsets.

4.5.2.7. Acknowledgements

This work was financially supported by the General Secretariat of Research and Technology (GSRT), Ministry of Development of Greece and by the Ministry of National Education and Religious Affairs of Greece through the "Pythagoras II" project.

4.5.2.8. References

Anderson, H., Jackson, J., 1987. Active tectonics of the Adriatic region. Geophys. J. R. astr. Soc., 91, 937-983.

Baker, C., Hatzfeld, D., Lyon-Caen, H., Papadimitriou, E., Rigo, A., 1997. Earthquake mechanisms of the Adriatic Sea and western Greece, Geophys. J. Int., 131, 559-594.

Benetatos, Ch., Kiratzi A., Roumelioti Z., Stavrakakis G., Drakatos G., I. Latoussakis, 2005, The 14 August 2003 Lefkada Island (Greece) earthquake: focal mechanisms of the mainshock and of the aftershock sequence. Journal of Seismology, 9, 171-190.

Blakely, R.J., 1981, A program for rapidly computing the magnetic anomaly over digital topography: U.S. Geological Survey Open-File Report 81-298, 46 p.

Gettings, M.E., Houser, B.B., 2000. Depth to bedrock in the Upper San Pedro Valley, Cochise County, southeastern Arizona, Open-File Report 00-138, Online version 1.0 (http://pubs.usgs.gov/of/2000/of00-138/).

Hansen, R. O., Wang, X., 1988. Simplified frequency-domain expressions for potential fields of arbitrary three-dimensional bodies: Geophysics, 53, 365-74.

Hildenbrand, T.G., 1983. FFTFIL: A Filtering Program Based On Two-Dimensional Fourier Analysis, U.S.G.S. Open -File Report P. 83-287.

Jackson, J., 1994. Active tectonics of the Aegean region. Annu. Rev. Earth Planet. Sci., 22, 239-271.

Kane, I., Assessment of geophysical structure of the crust in Albania using gravity and magnetic measurements, PhD thesis, Aristotle University of Thessaloniki, submitted 2003.

Kiratzi, A., 2002. Stress tensor inversions along the westernmost North Anatolian Fault Zone and its continuation into the North Aegean Sea. Geophys. J. Int., 151, 360-376.

Kiratzi, A., E. Louvari, 2003. Focal mechanisms of shallow earthquakes in the Aegean Sea and the surrounding lands determined by waveform modeling: a new database. "Journal of Geodynamics", 36, 251 - 274.

Lagios, E., S. Chailas, R.G. Hipkin, 1996. Newly compiled gravity and topographic databanks of Greece. Geophys. J. Int., 126, 287-190.

Louvari, E., 2000. A detailed seismotectonic analysis of the Aegean and the surrounding area, PhD thesis, Aristotle University of Thessaloniki, pp 374.

Louvari, E., Kiratzi, A., Papazachos, B. C., 1999. The Cephalonia Transform Fault and its continuation to western Lefkada Island. Tectonophysics , 308, 223-236.

Louvari, E., Kiratzi, A., Papazachos, B., Hatzidimitriou, P., 2001. Fault plane solutions determined by waveform modelling confirm tectonic collision in eastern Adriatic. PAGEOPH, 158(9-10), 1613-1638.

Makris, J., Stavrou, A., 1984. Compilation of gravity maps of Greece: Hamburg University, Institute of Geophysics, Hamburg, pp 12.

McClusky, S., Balassanian, S., Barka, A., Demir, C., Georgiev, I., Hamburg, M., Hurst, K., Kahle, H., Kastens, K., Kekelidze, G., King, R., Kotzev, V., Lenk, O., Mahmoud, S., Mishin, A., Nadariya, M., Ouzounis, A., Paradissis, D., Peter, Y., Prilepin, M., Reilinger, R., Sanli, I., Seeger, H., Tealeb, A., Toksoz, M.N., Veis, G., 2000. Global Positioning System constraints on plate kinematics and dynamics in the eastern Mediterranean and Caucasus. J. Geophys. Res., 105, 5695-5720.

Nabighian, M.N., 1972. The Analytic Signal of Two-Dimensional Bodies With Polygonal Cross-Section: Its Properties And Use For Automated Anomaly Interpretation. Geophysics, 37, 507-517.

Nabighian, M.N., 1984. Toward A Three-Dimensional Automatic Interpretation of Potential-Field Data via Generalized Hilbert Transforms: Fundamental Relations: Geophysics, 49, 780-786.

Papazachos, C. B., Hatzidimitriou, P. M., Panagiotopoulos, D. G., Tsokas, G. N., 1995. Tomography of the crust and upper mantle in southeast Europe. J. Geophys. Res., 100, 12405-12422.

Papazachos, C.B., Nolet, G., 1997. P and S deep velocity structure of the Hellenic area obtained by robust nonlinear inversion of travel times. J. Geophys. Res., 102, 8349-8367.

Papazachos C. B., Scordilis E., Peci, V., 2005. Crustal and Upper Mantle P- and S Velocity Structure of the Southern Adriatic-Eurasia Collision Obtained By Non-Linear Inversion of Regional Travel Times, Geophys. J. Int., (in press).

Papazachos, B.C., Comninakis, P.E., 1970. Geophysical features of the Greek Island Arc and Eastern Mediterranean Ridge. Com. Ren. Des Séances de la Conférence Réunie a Madrid, 1969, 16, 74-75.

Papazachos, B.C., Comninakis, P.E., 1971. Geophysical and tectonic features of the Aegean arc. J. Geophys. Res., 76, 8517-8533.

Papazachos, B.C., Papazachou, C., 2003. The earthquakes of Greece. Ziti Publications, Thessaloniki, Greece.

Papazachos, B.C., Papadimitriou, E.E., Kiratzi, A.A., Papazachos, C.B., Louvari, E.K., 1998. Fault plane solutions in the Aegean Sea and the surrounding area and their tectonic implication. Boll. Geof. Teor. App., 39, 199-218.

Papazachos, B.C., Mountrakis, D., Papazachos, C., Tranos, M., Karakaisis, G., A. Savvaidis, 2001. The faults that produced the known strong earthquakes in Greece from 5th century up to present. Proc. of the 2nd Conf. of Earthquake Engineering and Engineering Seismology, Thessaloniki 28-30 Nov. 2001, vol. 2, 17-26.

Parker, R. L., 1973. The Rapid Calculation of Potential Anomalies. Geophysical Journal of the Royal Astronomical Society, 31, 447-455.

Phillips, J.D., 1997. Potential-Field Geophysical Software for The Pc, Version 2.2. U.S. Geological Survey Open-File Report 97-725.

Phillips, J.D., 2001, Processing and interpretation of aeromagnetic data for the Santa Cruz basin – Patagonia Mountains area, south-central Arizona - a preliminary report: U.S. Geological Survey Open-File Report 15 p.

Roest, W. R., Verhoef, J., Pilkington, M., 1992. Magnetic interpretation using the 3-D analytic signal. Geophysics 57(1), 116-125.

Scordilis, E. M., Karakaisis, G. F., Karacostas, B. G., Panagiotopoulos, D. G., Comninakis, P. E., Papazachos, B. C., 1985. Evidence for transform faulting in the Ionian Sea: The Cephalonia Island earthquake Sequence of 1983. PAGEOPH, 123, 388-397.

Spakman, W., 1986. Subduction beneath Eurasia in connection with the Mesozoic Tethys. Geol. Mijnb., 65, 145-153.

Thurston, J.B., Smith, R.S., 1997. Automatic Conversion of Magnetic Data to Depth, Dip, and Susceptibility Contrast Using Spi ™ Method: Geophysics, 62 (3), 8-7-813.

Tsokas, G.N., Hansen, R., 1997. Study of the crustal thickness and subducting lithosphere in Greece from gravity data. Journal of Geophysical Research 102, 20585– 20597.

Tsokas, G.N., 2000. The Milos Island Bouguer anomaly revisited by means of a complex attribute analysis and inferred source parameter estimates. Journal of the Balkan Geophysical Society, Vol. 3, No. 4, p. 77-86.

Van Hinsbergen, D.J.J., van der Meer, D.G., Zachariasse, W.J., Meulenkamp, J.E., 2005. Deformation of western Greece during Neogene clockwise rotation and collision with Apulia, International Journal of Earth Sciences, DOI 10.1007/s00531-005-0047-5.